UNSUPERVISED SEGMENTATION ALGORITHM OF HRTEM IMAGES

Ainhoa Mendizábal[1], Julián Cabrera[2], Luis Salgado[3], Narciso García[4], Juan C. González[5]

[1,2,3,4] Grupo de Tratamiento de Imágenes
E.T.S. Ingenieros de Telecomunicación
Universidad Politécnica de Madrid
E-28040 Madrid - Spain
{amv, jcq,lsa,ngs}@gti.ssr.upm.es

[5] Dpto. de Ingeniería de Circuitos y Sistemas
E.U.I.T. Telecomunicación
Universidad Politécnica de Madrid
E-28040 Madrid - Spain
jcgsande@ics.upm.es

ABSTRACT

We propose a new *unsupervised* segmentation algorithm for high resolution transmission electron microscopy (HRTEM) images of nanocomposite materials. The proposed algorithm overcomes two major artefacts affecting these images, high level of noise and non-uniform illumination. The identification of the particles is based on the generation of a hierarchy of lower resolution images and a pixel-based segmentation at the highest level. The second part of the algorithm deals with the accurate determination of the border of the particles by means of snakes, and a final contour refinement through the hierarchy of images. The experimental results obtained over real HRTEM images show a good performance in terms of both, detection of particles and determination of their borders.

1. INTRODUCTION

Metal nanoparticles show special electrical, magnetic and optical properties interesting for applications such as chemical and biomedical sensors, selective solar or molecular absorbers, broadband polarizers or all-optical switches [1]. These properties change when the dimensions, separation or shape of the nanoparticles are modified. The determination of such geometric characteristics is usually done by analyzing images obtained with high resolution imaging techniques, such as transmission electron microscopy or atomic force microscopy.

A first step in this analysis consists of the image segmentation in order to separate the nanoparticles from the background. In most of the cases, these images are characterized by a high level of degradation, which makes the nanoparticles identification a non-trivial task. Currently, to overcome these problems, a manual (operator based) segmentation is carried out. Thus, there is a clear need for specific segmentation algorithms that eliminate the need of human operation while providing accurate segmentation results.

In this work, we focus on segmentation strategies for high resolution transmission electron microscopy (HRTEM) images of nanocomposite materials (consisting in metal nanoparticles embedded in a dielectric matrix). As will be seen, these images show a high level of noise and a non-uniform illumination. We propose a new unsupervised segmentation algorithm which is able to automatically identify the nanoparticles with a high degree of accuracy.

The outcome of our proposed algorithm allows further characterization of relevant geometrical features of the nanoparticles, such as: estimates of their size distribution, the average particles separation, their density, etc.

The rest of the paper is organized as follows: Section 2 describes the segmentation algorithm, Section 3 shows the results obtained, and Section 4 presents the main conclusions.

2. SEGMENTATION STRATEGY OVERVIEW

A block diagram of the proposed segmentation approach is presented in Figure 1. The input of the system is a full resolution HTREM image, I_0. The result of the algorithm is a segmented image, S_0, where nanoparticles have been separated from the background and different geometrical parameters can be accurately computed.

2.1 Pyramid generation

In order to remove the noise that is present in the test images, (Figure 2.a) we build a hierarchy of lower resolution images $\{I_0, I_1, \ldots I_L\}$ following a standard quad-tree approach [2]. Image I_{i+1} is obtained low-pass filtering (using a binomial filter) and subsampling I_i by two rows and columns. The high level of noise forced to use a binomial 9x9 filter and build a three level pyramid. Images at the third level, I_3, (see Figure 2.b) show a significant improvement in the contrast and definition of the particles. Moreover, images size has been reduced to 250x350 pixels, thus the computational requirement for the segmentation algorithms is significantly reduced.

2.2 Pixel based segmentation

The considered HTREM images present a non uniform illumination that has to be compensated in order to allow the application of further histogram thresholding techniques. A standard technique [3] has been used to correct the illumination. A coarse estimation of the image background illumination is computed. Image I_3 is divided into non-overlapping blocks and the maximum grey level in each one is selected as the background illumination representative. The size of these blocks has been determined experimentally to 12x12 pixels. A single value is obtained for each block, so, in order to obtain an auxiliary image with the same size, a bicubic interpolation is applied. This background illumination estimated image is then subtracted from the input image, I_3, correcting the illumination distortion.

0-7803-8554-3/04/$20.00 ©2004 IEEE.

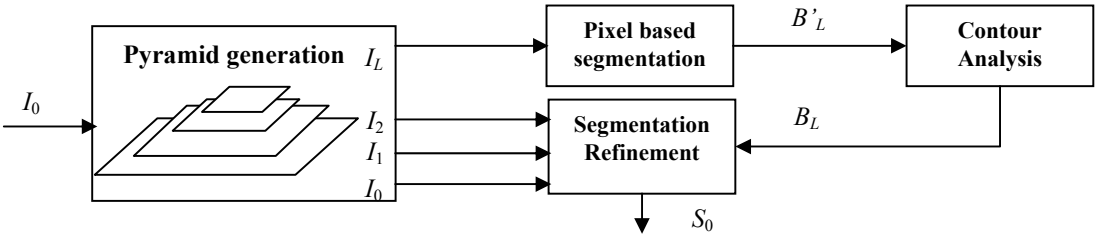

Figure 1. Segmentation strategy block diagram.

In Figure 3, it can be observed how the histogram of image I_3 (a) is modified after the illumination correction to show (b) a bimodal characteristic (particles correspond to dark values, while background corresponds to bright values), suitable for the application of a global histogram thresholding technique.

An unsupervised histogram global thresholding technique based on the work of Otsu [2] has been used to accurately segment the particles. The idea is to compute the threshold value, T, for which the weighted sum of group variances, σ^2_w, is minimized. σ^2_w is defined as follows:

$$\sigma^2_w = q_1(T) \cdot \sigma^2_1(T) + q_2(T) \cdot \sigma^2_2(T)$$

where $q_1(T)$, $q_2(T)$ represent the probability of a pixel to belong to each one of the histogram modes, and $\sigma^2_1(T)$ and $\sigma^2_2(T)$ are their variances. A sample of the segmentation result is presented in Figure 2.d.

2.3 Contour analysis

This processing phase works on those particles whose contours are not accurately fitted to their real borders as a result of the histogram based segmentation process. For this purpose, we consider the use of snakes as in [4][5].

From the segmented image previously obtained, we define an active contour as an ordered collection V of n points that define the edge of the particle:

$$V = \{v_1, v_2, ..., v_n\} \quad v_i = (x_i, y_i), \quad i = \{1, 2, ..., n\}$$

where (x_i, y_i) are the pixel coordinates of point v_i.

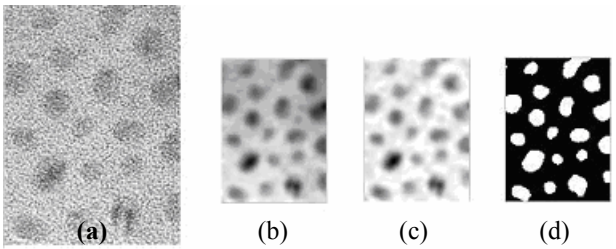

Figure 2. (a) Original image I_0, (b) Sampled & Low Pass filtered image I_3, (c) Illumination corrected image, (d) segmentation result.

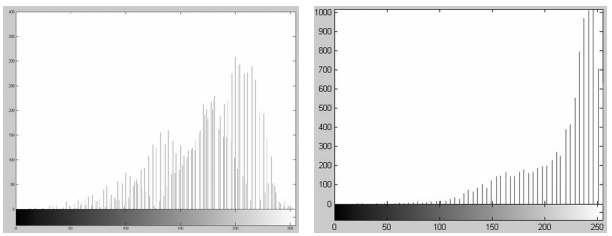

(a) (b)

Figure 3. (a) Histogram of I_3, (b) histogram after the illumination correction process.

The points of the active contour iteratively approach the target boundary through the solution of an energy minimization problem. The energy function in the neighborhood of any pixel of the contour is defined as follows:

$$E_i = a \cdot E_{\text{int}}(v_i) + b \cdot E_{ext}(v_i)$$

where E_i, E_{int}, and E_{ext} are matrices representing the energy values of the neighborhood of point v_i, and a, b, are constant weighting factors. The value at the center of each matrix corresponds to the energy at point v_i, while other matrix values correspond to the energy of pixels within the neighborhood.

Four different forces have been considered in the computation of E_i:

2.3.1 Internal Forces.

The internal energy function used herein is defined as follows:

$$E_{\text{int}} = c \cdot E_{con}(v_i) + d \cdot E_{bal}(v_i)$$

where c, d are constant weighting factors, E_{con} (continuity) coerces, in absence of other forces, a closed deformable contour into a circle, while E_{bal} (balloon) enforce the contour to expand.

The energy term for each element e_{jk} in the matrix E_{con} is defined as follows [6]:

$$e_{jk} = \frac{1}{l(V)} \left\| p_{jk}(v_i) - 0.5 \cdot (v_{i-1} + v_{i+1}) \right\|$$

$$l(V) = \frac{1}{n} \cdot \sum_{i=1}^{n} \left\| v_{i+1} - v_i \right\|^2$$

where p_{jk} is the pixel in the image that corresponds spatially to the energy matrix element e_{jk}, and $l(V)$ is a normalization factor.

The energy term for each element, e_{jk}, in the matrix E_{bal} is the dot product of

$$e_{jk}(v_i) = n_i \cdot \left(v_i - p_{jk}(v_i)\right)$$

where n_i is the outward normal vector of the contour at point v_i.

To adapt the balloon force so that it becomes stronger in homogeneous regions and weak near object boundaries, we coerce this force into varying inversely proportionally to the image gradient magnitude as proposed in [7].

2.3.2 External Forces

The external energy function is intended to attract the deformable contour to object boundaries.

$$E_{ext} = m \cdot E_{mag}(v_i) + g \cdot E_{grad}(v_i)$$

where m, g are constant weighting factors, E_{mag} (image intensity term) and E_{grad} (image gradient energy) attract the contour to regions of high intensity (background), and to edges in the image respectively. In order to avoid the attraction of the contour to the boundaries of other objects in the image, the gradient is calculated in the direction of the normal vector of the contour

The image intensity energy for matrix element e_{jk} is formulated as:

$$e_{jk}(v_i) = I(p_{jk}(v_i))$$

where $I(p_{jk})$ is the intensity of the pixel at position p_{jk} within the image. Finally, the image gradient energy for element e_{jk} is:

$$e_{jk} = -n_i \cdot \nabla I\left(p_{jk}(v_i)\right)$$

where n_i is the normal vector of the contour at v_i.

2.3.3 Describing the process

As a result of the creation process of the nanocomposite materials, the embedded particles are expected to show an ellipsoidal form. Nevertheless, it may occur that several particles combine resulting in an amorphous contour. We have applied the contour analysis only to those particles showing ellipsoidal forms.

Firstly, we approach each particle border obtained in the previous stage to an ellipsoidal form using the algebraic distance fit algorithm proposed in [8]. Only those particles whose resulting ellipses properly fit to their real shapes will be considered for the application of the snakes.

Then, we define an initial contour that is contained within the particle limits. For that purpose, we erode the considered particle with a circular mask and define its new boundary as the active contour.

For each pixel of the contour, we compute the aforementioned energies on a 3x3 neighborhood. For this computation we use a low pass filtered version of the image I_3 from the Pyramid Generation module, in order to reduce the noise of the image and avoid any artifact introduced by the illumination correction. The values of the weighting factors have been determined empirically and have been set for all the images to $c = 0.35$, $d = 0.3$, $m = 0$ and $g = 0.35$.

As can be observed, the energy function will comprise the continuity, the balloon, and the gradient terms while the intensity term is discarded. This result can be justified due to fact that the nanoparticles do not show a monotonic decrease in intensity, so the intensity term is not relevant for this type of images. On the other hand, the ellipsoidal form of the particles, and the definition of the initial contour within the particle limits is well characterized by the consideration of the continuity, balloon and gradient forces.

Then, the initial point of the contour is moved to the lowest energy point in the neighborhood. As described before, this process is repeated until a minimum energy state is reached.

2.4 Segmentation refinement

The objective of this module is, from the segmented image obtained at the lowest resolution level, B_L, generate the segmented image at the maximum resolution level, S_0.

The projection of image B_i to the next lower level, i-1, is performed as follows:

$$e(x, y, i-1) = e(\text{int}(x/2), \text{int}(y/2), i)$$

where $e(x,y,i)$ is the identification label (background or particle) for pixel (x,y) at level i, and int(.) is the integer part.

We define an *uncertainty area* [9], A(I_{i-1}), in the *i-1* level, which contains every pixel whose label differs from the label of any other pixel located in its 3x3 neighborhood. Formally,

$$A(I_{i-1}) = \{(x,y) \mid \exists (x_8, y_8) \in N_8(x,y) \mid e(x,y) \neq e(x_8, y_8)\}$$

where $N_8(x,y)$ represents the eight adjacent pixels to the considered pixel (x,y), (x_8,y_8) indicates any pixel of $N_8(x,y)$, and $e(.)$ the label associated to pixels at level i-1.

Thus, the objective is to classify each pixel within the uncertainty area according to the information of image I_{i-1}. For that purpose, we define a neighborhood of size $21 \cdot 4^{L-i-1}$ x $21 \cdot 4^{L-i-1}$ pixels for each pixel of $A(I_{i-1})$. The factor 4^{L-i-1} is used in order to maintain the proportionality between image and neighborhood sizes at each level of the pyramid. Then, using this neighborhood, a new threshold is automatically computed as described in section 2.2. If the intensity value of the pixel is lower or higher than the threshold value, it is labeled as a particle pixel or as a background pixel respectively.

Finally, due to the high level of noise, we have applied an opening with a five pixels radio disk in order to smooth the resulting borders.

3. RESULTS

The proposed algorithm has been tested over several real HTREM images (2000x2800 pixels) obtaining successful results.

Regarding nanoparticle identification, the pixel-based segmentation performed by the algorithm provides good results. False positives (detected non-existent particles) are less than 2%, and false negatives (undetected existent particles) do not occur.

In order to evaluate the improvement of the use of snakes in the contour analysis, we have compared the results of the proposed algorithm with and without the contour analysis process. Focusing on those particles whose segmentation results differ significantly in both approaches ($A \cap B / AUB < 75$ %, where A, B represent the resulting sets of pixels of a particle segmented by each approach), we have obtained that in the 85 % of the cases the result obtained using snakes is better, and only the 5% of them get worse results (in the 10% left there are no significant differences). Moreover, with the use of the snakes, the final contours of the particles are smoother due to the contribution of the continuity energy term. Figure 4 shows an example of the contour analysis process and Figure 5 shows an example of the final result for a particle (a) without using snakes and (b) including the contour analysis.

Finally, Table 1 shows a comparison of the results obtained by the proposed algorithm with those obtained by manual segmentation in terms of background and particle area. As can be observed, the difference ranges only from 2-8 %.

4. CONCLUSIONS

We have presented an unsupervised segmentation algorithm for HRTEM images of nanocomposite materials. The proposed algorithm overcomes two major artefacts affecting these images, high level of noise and non-uniform illumination, and provides accurate results in terms of both, detection of particles and determination of their borders. Thus, the outcome of our proposed algorithm allows further characterization of relevant geometrical features of the nanoparticles.

Test	Manual		Automatic		Diff.
	BG. area	Obj. area	BG. area	Obj. area	
1	70,93%	29,07%	73,15%	26,85%	2,21%
2	69,27%	30,73%	74,66%	25,34%	5,39%
3	66,04%	33,96%	72,10%	27,90%	6,06%
4	62,14%	37,86%	69,70%	30,30%	7,56%
5	64,29%	35,71%	67,94%	32,06%	3,66%

Table 1. Segmentation results related to Background/Object percentage areas.

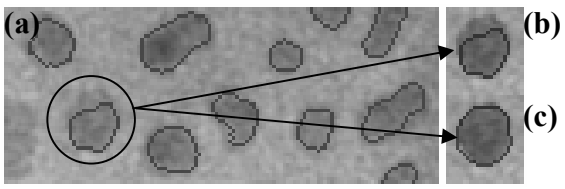

Figure 4. (a) Segmented image, (b) Particle contour mismatched, (c) redefined contour using snakes.

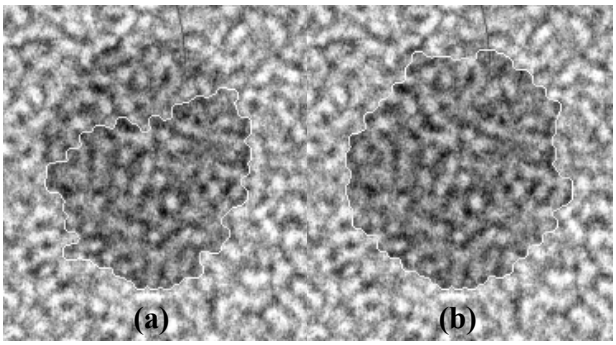

Figure 5. Segmented particle obtained at the full resolution image I_0. (a) Particle contour mismatched (c) redefined contour using snakes.

5. ACKNOWLEDGEMENTS

The authors would like to thank Dr. R. Serna and C. N. Alfonso from Instituto de Optica, Daza de Valdés, CSIC for providing the HRTEM images.

This work has been partially supported by the Comisión Interministerial de Ciencia y Tecnología of the Spanish Government under project TIC2001-3069 (ADREP3D).

6. REFERENCES

[1] A. Suarez-Garcia et al.. "Controlling the transmission at the surface plasmon resonance of nanocomposite films using photonic structures". Appl. Phys.Lett. 83, 1842-4, 2003.

[2] R M. Haralick, L.G. Shapiro, "Computer and Robot Vision" Volume I, Addison - Wesley Publishing Company, 1992.

[3] J.C.Russ, "The image processing Handbook", CRC Press, 1995.

[4] R. Luis-García et al., "A fully automatic algorithm for contour detection of bones in hand radiographs using active contours", in Proc. IEEE ICIP 2003, Vol III, pp. 421-424, Barcelona, Spain, 2003

[5] M.S Atkins, B. Mackiewich, "Fully automatic segmentation of the brain in MRI", IEEE Transactions on Medical Imaging, 17(1): 98-107, Feb. 1998.

[6] K. Fung Lai. "Deformable Contours: Modeling, Extraction, Detection, and Classification". PhD thesis, University of Wisconsin-Madison, Madison, Wisconsin, 1994.

[7] V. Chalana et al., "Integrating region growing and edge detection using regularitation" Proceddings of the SPIE Conference on Medical Imaging, SPIE, 1995

[8] E. Trucco et al. "Introductory techniques for 3-D computer vision. Prentice Hall, 1998.

[9] L. Salgado et al., "Efficient Image Segmentation for Region-Based Motion Estimation and Compensation", IEEE Trans. On Circuits and Systems for Video Technology, Vol. 10, Nr. 7, October 2000.